



Adding twists and turns to magneto-transport measurements

...with attocube tools: ANR, atto3DR and attoTMS

Sabrina Teuber, Luca Gragnaniello, Federico Valmorra, Mirko Bacani, Florian Otto
attocube systems AG, Haar, Germany

The characterization of materials exploring angle-dependent magneto-transport properties is one of the most widely used techniques in solid-state physics. For this, one requires not only a wide sample temperature range, from room temperature down to few Kelvins or below, but often also a powerful vector magnetic field. Therefore, precise control of the 3-dimensional field is of utmost importance for such investigations. However, conventional superconducting vector magnets are not only costly, but also limited in field strength: at least two directions over three typically cannot exceed one or two Tesla.

The renowned attocube expertise in nanopositioning has created an elegant solution to overcome this limit, by providing a broad portfolio of piezo-driven rotators, which are able to perform also in ultra-high vacuum and cryogenic conditions. Beyond single rotator units, attocube also provides a eucentric double rotator – the atto3DR, where the two axes of rotation intersect in the centre of the sample, which itself is sitting in the homogeneity center of the magnetic field. In this way, a strong one-dimensional magnetic field (e.g. 9 T or 12 T) becomes immediately accessible also in any other direction. Thus, it provides for example an equivalent of a 9 T-9 T-9 T vector magnet, which is as of yet impossible to manufacture. Moreover, it provides this equivalent for significantly lower costs than a regular vector magnet (such as 5 T-2 T-2 T), which is limited to rotating max. 2 T in 3D.

Finally, attocube also offers a fully integrated expert measurement platform: to simplify the work of scientists, especially those who are just starting their new lab, we took care also of the integration of the atto3DR into a complete measurement system, including the automated attoDRY2100 cryostat and an all-in-one acquisition electronics Nanonis Tramea™, with one dedicated software to ‘rule them all’. All this allows researchers to ignore tedious technicalities, while maintaining a maximum of versatility through a powerful measurement electronics and software, and to focus on what really matters: science!

This white paper is divided into three parts: first, we outline why sample rotation is a major advantage in magneto-transport measurements, then, we provide an overview of attocube’s solutions, and in the last section, we show application examples for all products.

1. Rotate your sample: here is why

Physicists, chemists and material scientists are on a relentless quest for new materials with desired properties. Novel materials arise almost daily and undergo various

characterizations. Mapping of the Fermi surface plays one of the central roles in characterization of materials, because correlating electronic structure with the properties of materials enables designing materials with a desired property - tuned for specific future applications.

There are three main established techniques for mapping the Fermi surface: angle-resolved photoemission spectroscopy (ARPES), measurements of (semi)classical angle-dependent magnetoresistance oscillations (AMRO), and measurements of quantum oscillations (QO). All three techniques require measuring of the sample in different directions, which means they all benefit from utilization of rotators. While samples in ARPES have to be well protected from magnetic fields, high magnetic fields are indispensable in transport measurements of AMRO and QO. For AMRO, one needs constant magnetic fields, whereas for QO, one needs to sweep the magnitude of magnetic field. Therefore, the advantage of rotators vs vector magnets becomes especially obvious in the case of demanding transport measurements, like QO and AMRO, and attocube can offer a readily developed automated solution (see Section 2.3) for them.

Shubnikov-de Haas effect [1], which describes oscillations in the longitudinal resistivity (i.e. parallel to an applied current), is commonly used to deduce the shape of the Fermi surface, but also allows to extract the 2D electron density and the effective mass of charge carriers. Schematic examples of 3D Fermi surfaces are shown in *Figure 1*. Strong magnetic fields lead to a quantization of energy levels of electrons, and the separation of these so-called Landau levels can be tuned by the magnetic field strength. Upon increasing the external magnetic field, the Landau levels cross, one by one, through the Fermi energy periodically, which directly leads to oscillations in the measured resistivity. In momentum space, one can also depict these as extremal orbits on the Fermi surface (shown in Figure 1a) in the plane perpendicular to the applied field. A fast oscillation stems from a large Fermi extremum, i.e. a “belly – B”, a slow oscillation in turn stems from a small Fermi extremum i.e. a “neck – N”.

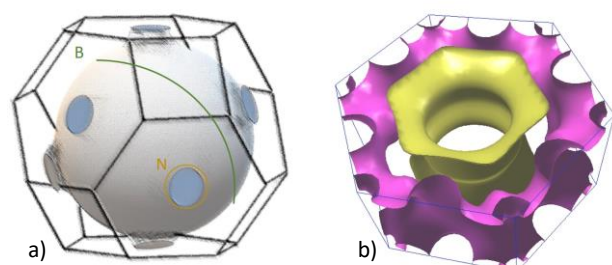


Figure 1: a) Fermi surface of Cu [2]. b) Fermi surface of Y [3].

As a general rule, Shubnikov-de Haas oscillations are periodic in $1/B$, where B is the magnetic field, and their amplitude grows with increasing B , and with decreasing temperatures. To map out the Fermi surface in 3D, precise control of the mutual



Adding twists and turns to magneto-transport measurements

...with attocube tools: ANR, atto3DR and atoTMS

orientation between field vector and sample surface is required.

More generally, being able to precisely control the field orientation in magneto-transport measurements helps to extract information on the properties of anisotropic samples. An example of a Fermi surface of an anisotropic sample is depicted in Figure 1b [3]. Majority of modern technologically interesting materials are anisotropic. Rotating the sample can particularly be useful in switching between in-plane and out-of-plane field configurations, or in precise alignment along a desired direction, e.g., along quasi 1-dimensional samples such as nanotubes or nanowires.

Piezo-driven nano-rotators effectively replace costly vector magnets and even enhance their performance, not only in maximum available field in an arbitrary direction, but also in capabilities for automated measurement routines. They are also superior to conventional mechanical rotators, which exhibit mechanical hysteresis. Moreover, when UHV conditions are needed, like e.g. in ARPES, piezo-rotators offer an additional advantage in comparison to mechanical rotators: no leaks of air inside the UHV chamber.

For symmetry reasons, and combined with field reversal through a bipolar magnet power supply, an angular range of 90° is in many cases sufficient. For piezo-rotators non-magnetic materials with low heat dissipation are used. Finally, a high precision and position stability of the angular motion in the m°-range translates into high resolution and good signal-to-noise of angle-dependent phenomena in anisotropic materials.

attocube rotators combine all those benefits.

2. attocube solutions

2.1. attocube ANR nano-rotators: how they work

attocube offers a broad portfolio of piezo driven nanopositioners, which also includes rotatory stages (attocube nano rotators - ANR). These are all based on the so-called slip-stick principle: the rotators typically feature a stationary base plate, which hosts a piezo drive element, linked to a moveable table by a finite holding force. When a sawtooth voltage is applied to the piezo, it first slowly expands, taking the table with it, and upon reaching the steep edge of the falling signal, the friction of the finite clamping force is overcome, resulting in a small net step ($\sim 1 \text{ m}^\circ$) along the direction of rotation. By periodic repetition, this allows for quasi-continuous macroscopic motion, at speeds of up to 30°/s at room temperature. Alternatively, the rotators can be driven in fine positioning mode via a DC voltage applied to the piezo, which allows for μm resolution over several m°. The slip-stick principle features another advantage besides its extreme precision: upon

reaching a desired target position, the piezo can be grounded to avoid electrical drift in position.



Figure 2: ANR portfolio [4]

The rotator portfolio covers a range of different sizes and orientations, as well as different material combinations suitable for cryogenic environments, ultra-high vacuum and/or high magnetic fields. Thanks to their small size, the rotators fit into most typical bore sizes of superconducting magnets; in fact, they have been used in fields of up to more than 30 T (see applications section).

Most models are also available with an encoder for position readout and closed loop control. All rotators feature a central aperture, through which measurement wires from a sample holder can be fed to facilitate motion over large angles with minimal strain.

Each rotator features two low-resistance wires for the drive signal, and three regular wires for the (optional) resistive encoder. To minimize the number of wires and hence the heat load in a cryostat when using more than one piezo-rotator or -stage, the ground and the sensor signal of the rotators/stages can be shared.

Since cooling power is always limited at cryogenic temperatures, let us briefly also take a closer look at the dissipated heat, which is generated by the friction-based working principle. The power P dissipated by a piezo is given by

$$P = C * U^2 * f * \tan(\delta)$$

where C is the piezo capacitance, U is the amplitude of the sawtooth supply voltage, f is the drive frequency, and δ is the so-called 'loss angle', and $\tan(\delta)$ the dissipation factor of the piezo material (typically 2% .. 4%). Drive voltage and frequency are hence the two parameters that the user can use to minimize the heat load, since the other two are given by the piezo material and rotator design. In a typical example at low temperatures, with $C=150 \text{ nF}$, $U=40 \text{ V}$, and $f=50 \text{ Hz}$, this yields $P=240 \mu\text{W}$. While this is of basically no concern at temperatures above 2 K for typical cryostats, reducing either the step size (by reducing the voltage), or the speed (by lowering the drive frequency) can significantly decrease the dissipated heat. To



Adding twists and turns to magneto-transport measurements

...with attocube tools: ANR, atto3DR and attoTMS

achieve ultimately low temperatures, careful filtering and thermalization of all measurement lines, as well as customized thermal anchoring adopted to the specific sample environment in a dilution refrigerator are typically required. Examples of ANRs used at mK temperatures successfully can be found in the applications section.

2.2. atto3DR: Emulating strong vector fields in 3D

The atto3DR double rotator features two independent rotators combined into one housing, thus providing access to the full magnetic field (e.g. 12 T) in all directions relative to the sample surface, as already outlined in the introduction.

The atto3DR is shown in *Figure 3*.

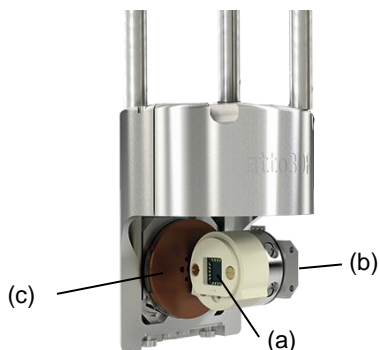


Figure 3: atto3DR: (a) sample holder with leadless ceramic chip carrier, equipped with 20 contacts; (b) the in-plane ANR; (c) the out-of-plane ANR. [4]

The sample is mounted and wire-bonded into a leadless ceramic chip carrier (LCCC) (a), equipped with 20 contacts, which are typically connected to just as many DC lines. The user can mount the LCCC onto the sample holder by using the two screws, which are visible on top of the lid.

An ANR positioner placed directly underneath the sample holder provides the in-plane axis of rotation (b). A second rotator adds the out-of-plane movement (c), which is both eucentric and completely independent on the in-plane rotation.

While the atto3DR was originally designed for the use in exchange gas, a customized version for cryogenic vacuum such as in dilution refrigerators is available on request; for application examples at mK temperatures, see the applications section.

2.3. Teaming-up your tools: attoTMS

The combination of variable temperatures and high magnetic vector fields, as required in magneto-transport measurements, have been hard to implement in a user-friendly fashion in the

past. Besides the difficulties associated previously with liquid cryostats, where the handling used to require experience and great care by the user, the sheer number of parameters which span the phase space of phenomena to be investigated calls for a massive automation of the measurement routines. For example, even the most basic measurements typically require recording resistance as a function of temperature, field and potentially one or several gate voltages. Hence, even just the software integration with all required instrumentation can be a time-consuming task for students and postdocs alike, which in the worst case is rewritten from scratch after every generation of students in every lab.

The attoTMS provides a transport-measurement solution for experts, combining user-friendliness and automation with versatility and unprecedented speed and signal quality. The system is based on the automated closed-cycle cryostat attoDRY2100 and integrates the above-mentioned 3D sample rotator atto3DR with a powerful measurement electronics, the Nanonis Tramea™.

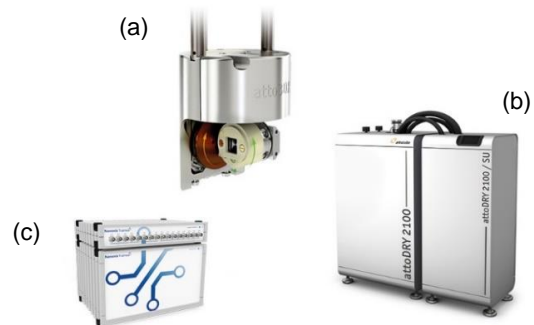


Figure 4: attoTMS package: a fully integrated all-in-one solution, combining atto3DR, attoDRY2100 and Nanonis Tramea™. [4]

The Nanonis Tramea™ includes up to 48 analog inputs and outputs, up to 8 lock-in modules, oscilloscopes and spectrum analyzers, a multi-functional user interface as well as several programming interfaces, incl. realtime scripting. Furthermore, the software integrates the automatic control of temperature (1.65 .. 300 K) and magnetic field (9 T or more) of the dry cryostat attoDRY2100, as well as an arbitrary orientation between sample surface and magnetic field direction given by atto3DR. Hence, generic n-dimensional sweeps of arbitrary parameters combined with data acquisition are easily possible with only one electronic device.

3. Scientific application examples

After outlining the key features and benefits of ANRs, the atto3DR, and the attoTMS, the last chapter of this white paper focusses on scientific results from transport measurements, which were facilitated by the use of our rotator solutions.



Adding twists and turns to magneto-transport measurements

...with attocube tools: ANR, atto3DR and atoTMS

3.1. ANR application examples

The following measurements were done using ANR rotators.

3.1.1 g-factor anisotropy examined in high magnetic fields and at 200 mK

In a collaboration of the Zumbühl Group (Basel, Switzerland) with RIKEN (Saitama, Japan), SAS (Bratislava, Slovakia) and UCSB (Santa Barbara, USA), an experiment for showing the separation of the isotropic and anisotropic g-factor corrections in GaAs quantum dots has been performed. The examination was done in two separate, lateral GaAs single-electron quantum dots. To experimentally determine the g-factor corrections, the spin splitting was extracted by measuring the tunnel rates for an in-plane magnetic field with various strengths and directions. The spin splitting defines the energy of the spin qubit and is one of the fundamental properties of a spin in a B-field. Here, they measure and separate the isotropic and anisotropic corrections to the g-factor in two GaAs devices, finding good agreement with recent theory. Beyond the well-established Rashba and Dresselhaus terms, the authors also identify a momentum-square-dependent Zeeman term g_{43} and a (smaller) term from the penetration into the AlGaAs barrier g_p [5].

This was done with the help of attocube rotator ANRv51: the sample was mounted on the piezo-driven rotator and precisely rotated in-plane of the magnetic field. Due to the resistive encoder for position readout, the rotator is the stage of choice for such setups. Moreover, the ANRv51 can be driven in magnetic-fields up to 35 T and used within cryogenic temperatures down to the mK range - this experiment was performed in a dilution refrigerator at an electron temperature of 200 mK and magnetic fields up to 14 T. Such field strengths, applied in an arbitrary in-plane direction, are only accessible with the rotator.

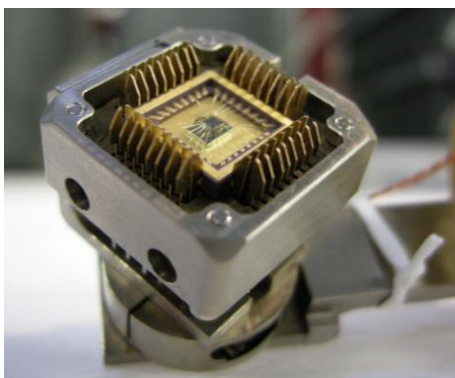


Figure 5: sample in chip carrier mounted on ANRv51

3.1.2 Angle-dependent transport measurements at 40 mK

Based on an attocube systems rotator ANR30/LT, a rotation stage for angle-dependent transport measurements in magnetic fields up to 33 T and temperatures down to 40 mK was built at the user facility of the High Field Magnet Laboratory in Nijmegen, Holland.

The mixing chamber of their dilution refrigerator offers only a limited space of 17 mm in diameter. Hence, the ultra-compact attocube rotator ANR30/LT is the positioner of choice for this task. The rotator is fixed on a plastic (Hysol) dilution refrigerator insert (shown in *Figure 6*). The angular movement of the ANR30/LT is transmitted via a thin copper wire (100 μ m diameter) to a rotating sample stage with a homemade 20-pin spring-contact socket for samples mounted into standard LCC-20 packages. The contacts are connected to a fixed 40-pin connector of the dilution refrigerator using copper wires with a diameter of 30 μ m to minimize the mechanical load on the rotator. The voltage pulses, which are needed for driving the rotator, are supplied via the same 40-pin connector using two parallel wires for each contact. Due to the small capacitance of the ANR30/LT of only 14 nF at low temperatures, the relatively high resistance of the cabling of approx. 36 Ohm in total does not raise a problem for the rotator.

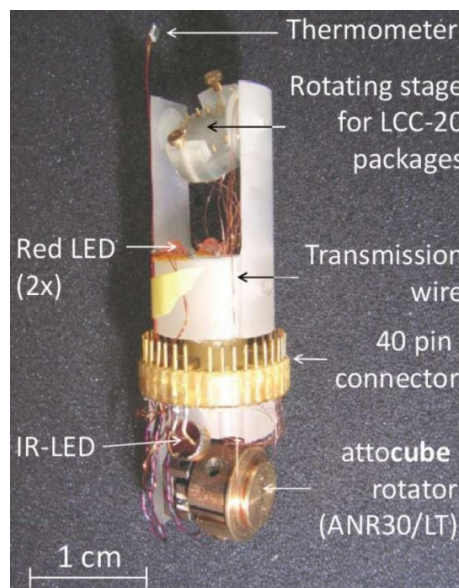


Figure 6: Setup for angle dependent transport measurements with an attocube rotator ANR30/LT which is inserted in a dilution refrigerator.

A GaAs-heterostructure Hall-bar was mounted onto the described insert and the angle-dependent Quantum Hall Effect between 0 and 52 degrees was measured at a temperature of 40 mK (see *Figure 7*). The angle covers a range from +110 degrees to -50 degrees, only limited by the contact wires' mechanical load [6].



Adding twists and turns to magneto-transport measurements

...with attocube tools: ANR, atto3DR and attoTMS

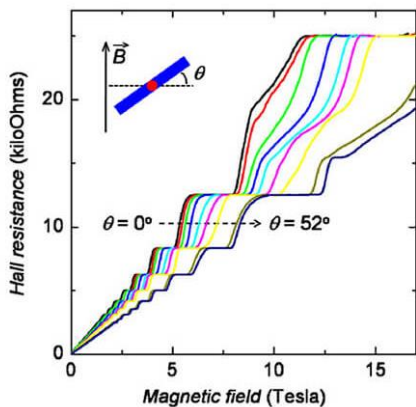


Figure 7: Angle dependent measurements of the Quantum Hall Effect in an AlGaAs two-dimensional electron gas.

3.1.3 Piezo-driven sample rotation system with ultra-low electron temperature

While dilution refrigerators readily provide temperatures down to 10 mK or less, the actual effective sample temperature is determined by the electron temperature. Due to the minuscule cooling power at such temperatures, and the finite heat leaks caused by the environment and the measurement wires themselves, as well as the lack of sufficient electron-phonon coupling, the electron temperature is often much higher (i.e. at 100 K or more).

At Peking University (Beijing, China), Dr. Pengjie Wang & co-workers in the Xi Lin group have carefully implemented the beryllium-copper version of the ANR101 positioner with resistive readout together with home-built thermal links and contacts, as well as homemade filters. This enabled them to achieve electron temperatures as low as 25 mK in their sample, while maintaining the ability to rotate by more than 90° in the field of a 10 T magnet, with a readout resolution of $\pm 0.02^\circ$, and a stability of $\pm 0.05^\circ$.

The rotator module is mounted to an insertable probe of a Leiden CF-CS81-600 dilution refrigerator. Thanks to the large sample space of 81 mm in diameter, a homemade sample holder for up to 4 samples with max. size of 5 mm by 5 mm is installed. It also features a red LED to illuminate samples at 4 K for higher charge carrier mobility. The cooling power of the probe is about 340 μW at 120 mK, which allows for continuous rotation at < 200 mK (60 V, 4 Hz, 300 nF). The sample can be changed within 10 hours from 50 mK to 50 mK.

In order to precisely determine the effective electron temperature, the group used a high mobility 2DEG sample, and measured the temperature dependence of the longitudinal resistance minimum in the thermally activated regime of quantum Hall states. The result deduced from an Arrhenius plot of the 7/2 FQH state clearly indicates a lowest temperature of 25 mK.

In an application example, the group investigated the tilt-induced localization and delocalization of the same sample in the second Landau level, for which a pressurized liquid ^3He cell had been necessary elsewhere [7].

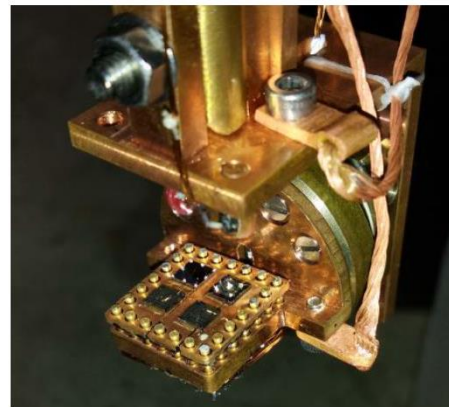


Figure 8: Rotator assembly with L-shaped sample holder, 4 mounted samples, and home-built thermal links.

3.1.4 Spin relaxation record at 25 mK and within high magnetic fields

Spin qubits based on quantum dots are promising candidates as building blocks for future quantum computers. In 2018, an international collaboration (Basel, Saitama, Tokyo, Bratislava and Santa Barbara) successfully demonstrated a new mechanism for electron spin relaxation for the first time experimentally, 15 years after this phenomenon has theoretically been predicted [8].

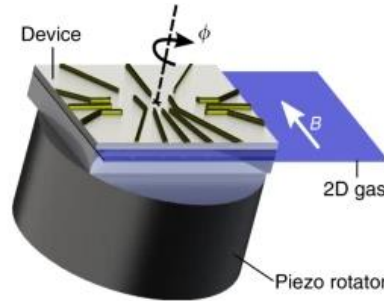


Figure 9: Measurement setup with sample on an ANRv51 for rotating around the angle φ in the plane of the magnetic field.

Working at 25 mK DR and in up to 14 T, a new record of electron spin lifetime of over a minute in a semiconductor nanostructure - GaAs - was achieved at around 0.6 T. More about this record can be found at [9].

For this setup attocube encoded ANRv51 was used as it perfectly fits the requirements of a mK temperatures and high magnetic fields system. Moreover, the sample of a single-electron quantum dot formed in a GaAs 2D electron gas could



Adding twists and turns to magneto-transport measurements

...with attocube tools: ANR, atto3DR and atoTMS

perfectly be aligned arbitrarily to the in-plane magnetic field with respect to the crystal axis.

3.1.5 Angle-dependent characterizations of materials at mK temperatures

The group of Anne de Visser at the Van der Waals - Zeeman Institute (University of Amsterdam, NL) has used two setups with an ANR51 and an ANRv220 for angle dependent transport measurements, both in a closed loop configuration.

In their first experiment, magneto transport measurements as a function of the angle θ in the trigonal basal plane of the topological superconductor $\text{Sr}_x\text{Bi}_2\text{Se}_3$ revealed a large two-fold anisotropy of the upper critical field B_{c2} . Such a rotational symmetry breaking of $B_{c2}(\theta)$ cannot be explained with standard models, and indicates unconventional superconductivity with an exotic order parameter. More about this work can be found at [10].

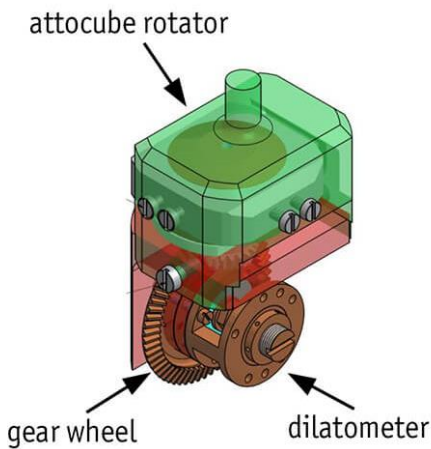


Figure 10: Graphical illustration of the setup with attocube ANR.

In the second setup, a home-built compact dilatometer was mounted on the ANRv220 in a dilution refrigerator. This was used to measure the anisotropy in the ferromagnetic and superconducting phase diagram of a single crystal of UCoGe by applying magnetic fields up to 14 T along the different crystallographic axes [11].

3.1.6 Transition from slow Abrikosov to fast moving Josephson vortices

Philip Moll & co-workers (ETH Zurich, Switzerland) observed the formation of fast moving Josephson vortices, which depends critically on the angular alignment. The especially challenging transport experiment in a liquid Helium cryostat required millidegree rotational accuracy and perfect angle stability over a wide range of temperatures (80 K - 2 K) and magnetic fields (± 14 T), far beyond the capabilities of other rotators. Using an ANR31, they were able to rotate the sample below 2 K with

better than 0.1° precision and could observe no drifts while sweeping temperature and magnetic field. Moreover, the precise nano-rotator setup was designed to fit on a small (25 mm diameter) standard sample carrier (see Figure 11). It performed extraordinary well, extending the capabilities of research into areas where extreme angular precision and stability are required.

The mobility of magnetic vortices in the layered superconductor SmFeAs(O,F) was studied and an enormous enhancement of vortex mobility was shown associated with a transition of the vortex nature itself, changing from Abrikosov to Josephson [12]. A perfectly in-plane Josephson vortex, centered in a “non-superconducting” Sm(O,F) layer, can only be weakly pinned and thus experiences the mentioned enhancement in mobility. This feature, however, is immediately lost if the field is tilted out of the FeAs planes and even the smallest misalignment (< 0.1°) completely destroys the effect as the misaligned vortex is not parallel to the crystallographic layers anymore. As mobile vortices cause dissipation, their mobility is observed as a very sharp spike in voltage as shown in Figure 12)

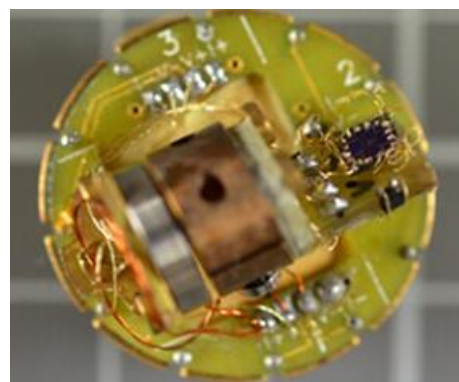


Figure 11: Rotator setup showing the ANR31/LT rotator carrying the sample and two Hall sensors.

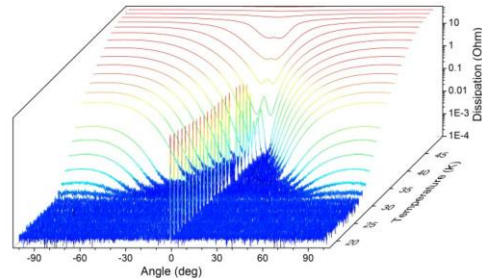


Figure 12: Flux-flow dissipation as a function of the angle between the magnetic field ($H = 12$ T) and the FeAs layers ($= 0^\circ$) for several temperatures.



Adding twists and turns to magneto-transport measurements

...with attocube tools: ANR, atto3DR and atoTMS

3.1.7 Ultra-low heat dissipating rotation system for quantum transport analysis

In 2010 L.A. Yeoh et. al. from the University of New South Wales (Sydney, Australia) analysed the quantum transport in semiconductor nanodevices. Their main goal was to achieve a suitable rotating system to study anisotropic Zeeman spin-splitting. In order to fully examine this effect, a precise rotation of the sample towards a magnetic field (up to 10T) is needed while maintaining a temperature below 100mK. The sample exists of AlGaAs/Ga/As heterostructures mounted in ceramic LCC20 device packages. Two copper wires are attached to the carrier.

Using the ANRv51 with RES encoder for position readout, the group designed a sample holder with two alternative mounting orientations (see *Figure 13*): one with in-plane rotation, and one with out-of-plane rotation of the chip carrier (see images). The ANRv51 is a perfect fit for this application: made from non-magnetic materials, it is fully mK compatible, and features a small aperture to feed the 20 copper wires to the backside of the rotator.

In their paper, the group carefully characterized the heat dissipation of their rotator as a function of rotation speed for different drive voltages and frequencies [13]. At slow rotation speeds, the heat dissipation could be kept to a minimum, allowing for temperatures below 100 mK even for continuous rotation. The time for relaxation back to the base temperature of 25 mK was found to be around 20 min. In addition, thanks to the slip-stick principle, the rotators can be grounded upon reaching a final target position, which ensures position stability and zero heat dissipation.

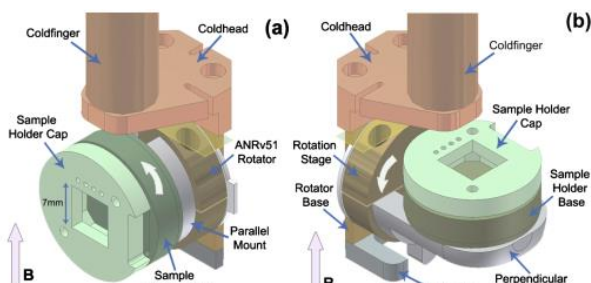


Figure 13: Rotation system assembly for rotating the sample in two separate configurations with respect to the applied magnetic field B .

3.2. atto3DR application examples

In this section, we present results using the atto3DR.

3.2.1 Van der Waals heterostructure under rotation at 40 mK

Understanding the mechanism of high temperature (high T_c) superconductivity is a central problem in condensed matter physics. Van der Waals heterostructures provide novel materials as model systems for quantum phenomena. An international collaboration (Berkeley, Stanford, Shanghai, Tsukuba, Seoul) reports in Nature signatures of tunable superconductivity in these special heterostructures, detected via a sharp drop in the resistivity and a plateau in the I-V curve below 1 K [14].

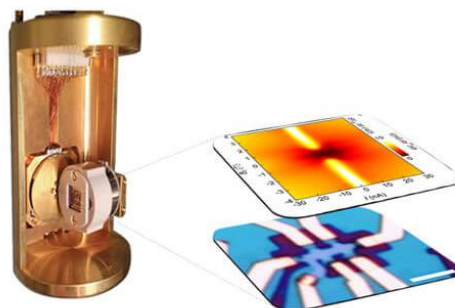


Figure 14: atto3DR for mK application with two images.

The transport measurements are performed in a dilution cryostat with a base temperature of 40 mK achieved through careful filtering. For in-plane measurements, the atto3DR double sample rotator was used, which conveniently allows for using the full field of a single solenoid in an arbitrary orientation. The authors find transitions from the candidate superconductor to Mott insulator and metallic phases, proving that the TLG/hBN superlattice provides a unique model system to study the triangular Hubbard model and its relation to unconventional superconductivity as well as potentially novel electronic states.

3.2.2 Cryogenic angle-dependent magnetoresistance measurement

Due to the arbitrary orientation inherent to self-assembled materials on the substrate, typical characterization techniques such as magnetoresistance measurements conducted at cryogenic temperatures greatly benefit from the possibility to freely change the mutual orientation of an external magnetic field and sample. Although this is easily possible e.g. by using a 3D vector magnet setup, the associated costs ($>> 100$ k\$) are often prohibitive. Single axis sample rotator setups on the other hand not only require choosing either an out-of-plane or in-plane configuration prior to cool down, but also put firm restrictions on certain measurements which rely on a precise orientation of the field e.g. perpendicular or parallel to an initially unknown direction along a sample structure. The



Adding twists and turns to magneto-transport measurements

...with attocube tools: ANR, atto3DR and attoTMS

perfect solution to such applications is attocube 3-dimensional rotator atto3DR.

Similar to a recent publication by C. H. Butschkow and co-workers from the group of Prof. Dieter Weiss (Univ. of Regensburg), magneto-transport measurements on individual GaAs/(Ga,Mn)As core-shell nanowires (see *Figure 15*) have been conducted [15].

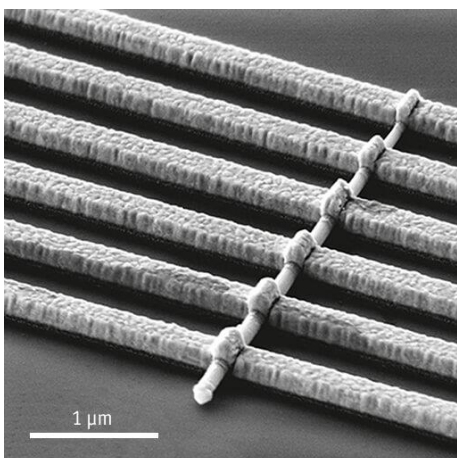


Figure 15: Magneto-transport measurements on individual GaAs/(Ga,Mn)As core-shell nanowires.

Figure 16 shows magnetoresistance at 5 T as a function of the angle between externally applied magnetic field and the nanowire axis for different rotation planes. in-plane rotation (orange), referring to the SiO₂ substrate plane, (green) out of plane (perpendicular) rotation with the long nanowire axis (typically 4 μm long and 100 nm in diameter) entirely in the rotation plane, and (blue) out of plane (transversal) rotation with the rotation plane transversal to the nanowire axis.

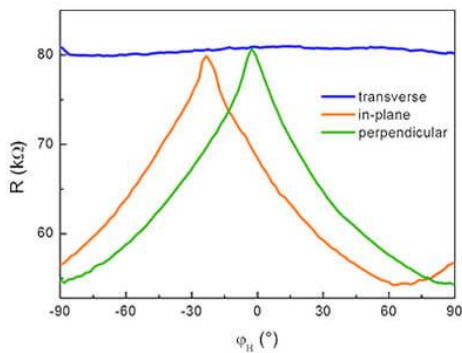


Figure 16: Magnetoresistance at 5 T as a function of the angle between externally applied magnetic field and the nanowire axis for different rotation planes.

3.2.3 Orbital ferromagnetism in twisted bilayer graphene below 30 mK

Van der Waals heterostructures, particularly in the form of magic-angle twisted bilayer graphene (tBLG), are one of the hottest topics in today's solid state physics research. While previous measurements on tBLG already indicated ferromagnetism as deduced from a large hysteretic anomalous Hall effect, and subsequently pointed to a Chern insulator, A.L. Sharpe and co-workers now experimentally showed via transport measurements that the ferromagnetism in tBLG is highly anisotropic, and suggests to be of purely orbital origin - which was never observed before [16].

For their measurements, the group mounted a sample of tBLG encapsulated in boron nitride flakes onto attocube atto3DR double rotator, working at electron temperatures down to less than 30 mK facilitated by careful filtering, and in magnetic fields of up to 14 T. A dedicated in-situ calibration of the tilt angle using the Hall resistance allowed for accurate control of the exact in-plane and out-of-plane orientations during their experiments.



Figure 17: Angular dependence of hysteresis loops in twisted bilayer graphene, measured with atto3DR at < 30 mK.

3.3 Shubnikov-de Haas oscillations measured with attoTMS

As explained in the first part, the Shubnikov-de Haas effect is an oscillation of the resistivity of a material, which occurs at low temperature as a function of the applied magnetic field. It appears in form of short and large oscillations, originating in momentum space respectively from large and small Fermi extrema of the 3D Fermi surface, as depicted in *Figure 1*. This effect allows determining the effective mass of charge carriers in the material.



Adding twists and turns to magneto-transport measurements

...with attocube tools: ANR, atto3DR and attoTMS



Figure 18: Nanonis Tramea™ – attoTMS software overview.

Here, we would like to take advantage of this known phenomenon, to show with a simple test some of the many assets of the attoTMS.

The attoTMS gives the possibility to easily control all the parameters of a magneto-transport measurement setup with an intuitive yet all-embracing modular software, like shown in *Figure 18*.

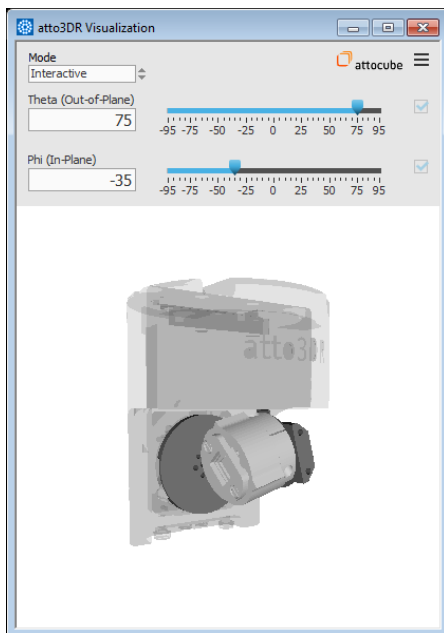


Figure 19: atto3DR Visualization tool in the software

The software has the capability to master the whole experiment: not only fast and powerful signal generation and acquisition with up to eight lock-in modules, but also a fine and programmable control of the sample temperature, the magnetic field and the in- and out-of-plane sample orientations. Each of these features has been developed in dedicated modules, which can be opened only when used and organized accordingly to the user preferences on the display. For example, current and possible orientations of the sample can be visualized with a clear tool, simulating the atto3DR movements in all the aspects, see *Figure 19*.

One of the many advantages of the attoTMS is to simplify the measurement and strongly reduce acquisition time. In our demonstration test, we mounted in an attoTMS a GaAs/AlGaAs 2DEG Hall bar sample, kindly provided by the group of prof. Adam Micolich from the University of New South Wales of Sydney, whose schematic is depicted in *Figure 20*.

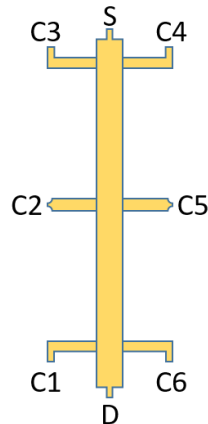


Figure 20: Schematic of the GaAs/AlGaAs 2DEG Hall bar sample used for this demonstration. The labels indicate the available contacts.

After cooling down at the base temperature, 1.7 K, we applied a constant DC current through the bar ($1 \mu\text{A}$), between S and D, while measuring the longitudinal (C3-C1) and transverse (C3-C4) resistance as a voltage drop between the contacts.

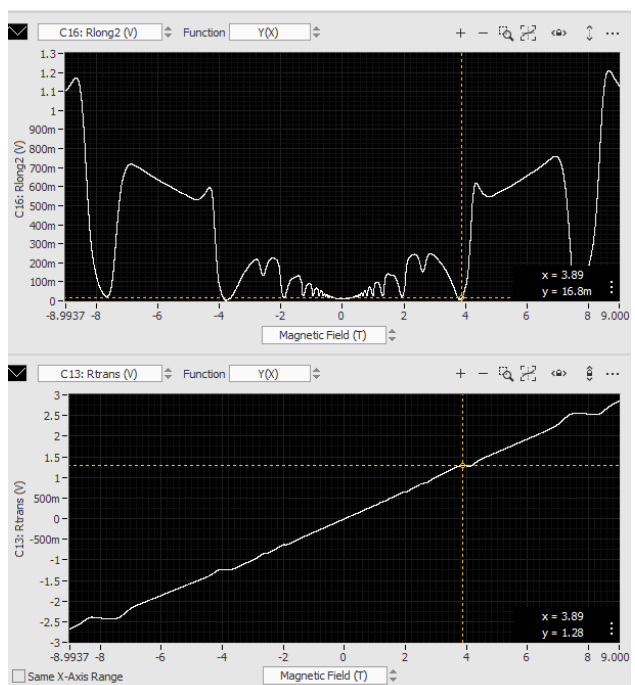


Figure 21: attoTMS measurements. Longitudinal (C3-C1) and transverse (C3-C4) resistances acquired during the sweep of the magnetic field, in the out-of-plane direction. The dashed red lines guideline the two curves.



Adding twists and turns to magneto-transport measurements

...with attocube tools: ANR, atto3DR and attoTMS

We first performed a classical measurement, by sweeping the magnetic field from -9 to +9 Tesla, while keeping the atto3DR out-of-plane rotator perfectly at 0°, thus applying a variable magnetic field perpendicular to the sample surface.

The resulting longitudinal (C3-C1) and transverse (C3-C4) voltage drops are plotted in *Figure 21*, as they appear in the attoTMS software.

As expected, the longitudinal voltage drop, which is proportional to the longitudinal sample resistance, is symmetric with respect to the magnetic field (horizontal axis) and displays the fast and slow oscillations of the Shubnikov-de Haas (SdH) effect. The transverse voltage drop presents plateaus at the corresponding magnetic field of the minima of the longitudinal curve, as highlighted by the dashed red guidelines.

By plotting the SdH as a function of the inverse of the applied magnetic field (*Figure 22*), it is possible to derive the sheet charge density.

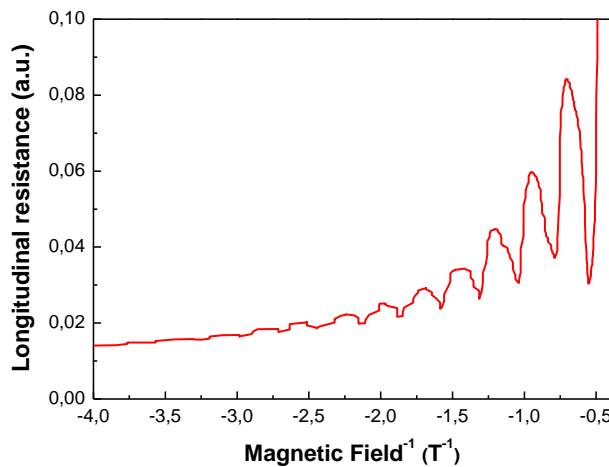


Figure 22: attoTMS measurements. Shubnikov-de Haas oscillations of the GaAs/AlGaAs 2DEG Hall bar as a function of the inverse of the magnetic field.

In this case, we found the sheet carrier density to be $1.88 \cdot 10^{11}$ el/cm²; with a mobility of: $3.04 \cdot 10^6$ cm²/Vs, and the lowest filling factor being equal 1.

A similar value, $1.90 \cdot 10^{11}$ el/cm², can be inferred by the slope of the transverse signal (Hall Voltage), thus showing a good consistency.

So far, we have only used the capability of the attoTMS to control signals, magnetic field and sample orientation with one unique software, without having yet exploited the advantage that rotating the sample can offer even in such a standard case. Indeed, the measurements described here above took 117 minutes, due to the slow capability of a highly inductive magnet to sweep the magnetic field.

Thus, we can now acquire the same signals, i.e. longitudinal and transverse resistance in constant DC 1 μA current, by sweeping the out-of-plane angle (θ) while keeping the magnetic field fixed at 9 T.

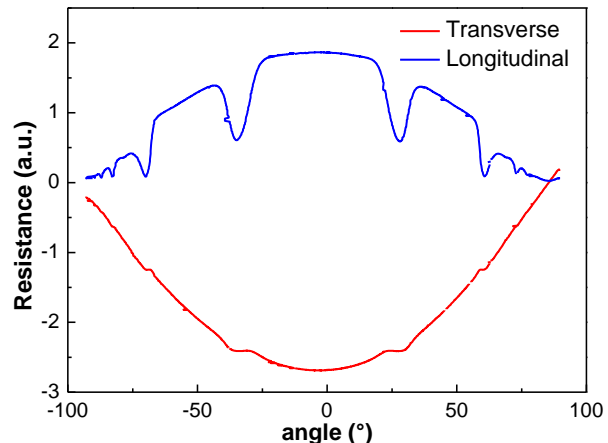


Figure 23: attoTMS measurements. Longitudinal (C3-C1) and transverse (C3-C4) resistances acquired at 9T while sweeping the out-of-plane angle (θ).

If we now plot the same data as a function of the effective magnetic field on the surface, i.e. $B \cos\theta$, where θ is the angle between the magnetic field and the normal to the surface, we obtain the same plot as for a magnetic sweep, including SdH oscillations. This should not surprise. Indeed, by rotating the sample we have actually swept the out-of-plane magnetic field from 0 ($\theta = 90^\circ$) to 9 T ($\theta = 0^\circ$). The difference? It took us only 24 minutes!

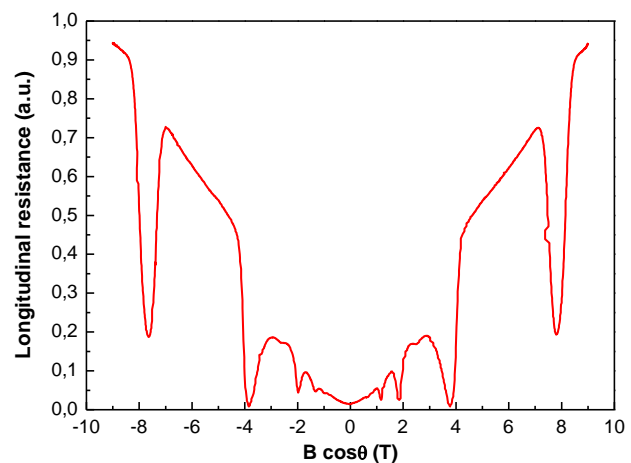


Figure 24: attoTMS measurements. The same data of the Figure 23 for the longitudinal voltage drop, plotted as a function of the effective magnetic field, $B \cos\theta$.

This is just a simple example of the capability of the attoTMS but the potential of this goes far beyond that. We are already looking forward what the attoTMS can enable you to do!



Adding twists and turns to magneto-transport measurements

...with attocube tools: ANR, atto3DR and attoTMS

4. Summary

Magneto-transport measurements typically involve variable temperatures, and high magnetic fields. Being able to rotate the sample is a key prerequisite to extract useful information such as 3D Fermi surfaces, effective mass and density of charge carriers, or many other parameter associated with the anisotropy of bulk materials, thin films, or mesoscopic structures. The use of piezo based sample rotators also helps to reach higher vector fields than achievable with vector magnets, to save costs, and to automate extensive sets of parameter sweeps. Hence, attocube ANRs and vertically integrated solutions thereof - atto3DR and attoTMS - constitute substantial advantage for every researcher who employs electrical measurements at cryogenic temperatures with a field dependence.

Contact our sales team for more information on how we can help you boost your efficiency!

5. References

- [1] L.W. Shubnikov, W.J. de Haas, Proc. Netherlands Roy. Acad. Sci. 33, 130 (1930)
- [2] Fermi Schematics, Sabrina Teuber, attocube systems AG
- [3] <http://www.phys.ufl.edu/fermisurface/>
- [4] [attocube systems AG](#)
- [5] [L.C. Camenzind et al., Phys. Rev. Lett. 127, 057701 \(2021\)](#)
- [6] [U. Zeitler et al., attocube Application Note CI04 \(2014\)](#)
- [7] [P. Wang et al., Rev. Sci. Instrum. 90, 023905 \(2019\)](#)
- [8] [L.C. Camenzind et al.; Nat Commun 9, 3454 \(2018\)](#)
- [9] <https://www.unibas.ch/en/News-Events/News/Uni-Research/New-mechanism-of-electron-spin-relaxation-observed.html>
- [10] [Y. Pan et al., Sci. Rep. 6, 28632 \(2016\)](#)
- [11] [A.M. Nikitin et al., Phys. Rev. B 95, 115151 \(2017\)](#)
- [12] [P.J.W. Moll et al., Nature Mater. 12, 134 \(2013\)](#)
- [13] [L. A. Yeoh et al., Rev. Sci. Instrum. 81, 113905 \(2010\)](#)
- [14] [G. Chen et al., Nature 572, 215 \(2019\)](#)
- [15] [C. Butschkow et al., Phys. Rev. B 87, 245303 \(2013\)](#)
- [16] [A.L. Sharpe et al., Nano Lett 2021, 21, 10, 4299 – 4304 \(2021\)](#)